Intercomparisons of Site VSWR Measurement Methods using Mode Filtering, Time Domain and Spatial Sampling Techniques

Zhong Chen
ETS-Lindgren
1301 Arrow Point Drive, Cedar Park, TX, USA
zhong.chen@ets-lindgren.com

Stuart Gregson
Next Phase Measurements
11521 Monarch St, Garden Grove, CA, USA
stuart.gregson@npmeas.com

***Abstract*—The validity and viability of using frequency domain mode filtering to qualify an EMC chamber above 1 GHz has been demonstrated in a previous study [1]. The novel approach overcomes the difficulties with under sampling encountered in the traditional spatial sampling method adopted by CISPR, and it also has the distinct advantage over the time domain method adopted by ANSI C63.25.1 in that broadband and low ring-down antennas are not required. In this study, we further examine one of the assumptions made in the previous study to translate the quasi-far-field pattern to the rotation center. The approximate method is compared to a more rigorous method by using a quasi-far-field to far-field transformation first before applying the phase translation and subsequent mode filtering. In this paper, we further validate the method by conducting an intercomparison study based on measurements conducted in a 3 m anechoic chamber to show the correlations of the mode filtering method to the CISPR and the time domain (TD SVSWR) methods. We demonstrate how the proposed method improves the test repeatability, lowers measurement uncertainties, and increases measurement efficiencies.**

***Index Terms*—EMC, SVSWR, Mode Filtering, Cylindrical Mode Coefficient.**

I. Introduction

In a previous study [1], the authors introduced a novel approach to measure the standing waves in an EMC anechoic chamber by using a cylindrical mode based filtering technique. Traditional SVSWR method adopted by the CISPR standards [2] tends to under sample the standing wave because only 6 points are taken along a 40 cm linear line to locate the maximum and minimum values of the standing wave. Additionally, VSWR is only measured for the cardinal points in the quiet zone (QZ). Time domain SVSWR [3] was developed to overcome some of these shortcomings by using a broadband antenna and time domain transformation (TD) to separate the multipath reflections from the main antenna responses, rather than relying on spatial movements of the antenna. Because the TD method requires broadband antennas with short ringdown times, it limits the applicability of the method in some cases. Besides, the TD method has not addressed the issue that VSWR is measured only for the cardinal points. Unlike the traditional CISPR method, which requires moving the antenna along a linear path, the mode filtering method measures the standing waves along the perimeter of the QZ, for which a dense sampling around the circle can be easily accommodated due to the ubiquity of an automated turntable in EMC chambers.

The mode filtering method is self-referencing in that there is no need to measure the radiation pattern of the measurement antenna separately. For SVSWR measurements, an omni-directional antenna is stipulated by the standards in order to adequately illuminate the chamber under test. The Remote Sensing Antenna (RSA) is set at a fixed position boresighted to the center of the QZ, *e.g.*, at 3 m away from the front edge of the QZ. The measurement antenna is placed at the outer edge of the QZ, and a single cut pattern data set is collected. The antenna pattern is then mathematically translated back to its rotation center, after which, the antenna cylindrical mode coefficients are computed. The cylindrical modes associated with the measurement antenna are now confined to the lower orders encompassing just the antenna, rather than the much larger QZ radius. Meanwhile, the modes associated with the chamber multipath effects do not get translated coherently and remain spread to the higher order modes. This provides a separation between the antenna modes and modes associated with the range multipath. The underlying antenna pattern can therefore be filtered and extracted with minimal impact from the chamber. With the reference antenna pattern recovered, the standing waves can be calculated by comparing the uncorrected pattern to the reference pattern without the need for further, auxiliary, measurements.

Mode filtering [4,5,6] is a well-established technique for antenna pattern measurements. The application to chamber QZ qualification is a natural extension. There are several unique challenges for applying the method to EMC chamber testing. Firstly, the frequency requirement for 1 GHz maybe at the lower end of the applicable range for mode filtering. Secondly, the measurement distance (typically 3 m) is perhaps too close to be considered the true far-field. In the far-field, only a differential phase shift is needed to translate the antenna from an offset

position to the center of the measurement coordinate system. For the finite range length application, this may be insufficient. Thirdly, since the CISPR SVSWR method is well established, the new method must correlate and allows for the establishment of a similar severity level for a test chamber. To this end, the study in [1] examined and adapted the algorithm to address these factors. The authors showed that the mode filtering method is not only feasible for the SVSWR application, but also effective in overcoming the shortcomings of the other two methods.

The intention of this paper is to validate the mode filtering method further from several aspects. First, to validate the geometric optics (GO) based centering scheme which was used to translate the antenna back to the rotation center [1], an alternative more rigorous algorithm is utilized as a first step to transform from the quasi-far-field to the true asymptotic far-field. The transformed far-field pattern is then moved to the center through the rigorous far-field phase shifting, where no approximation is needed. The rest of the processing is performed as in [1]. By demonstrating that each method produces equivalent results, this would further validate the ray-based treatment in [1]. Note that the rigorous quasi-far-field to far-field approach would require a denser angular sample spacing because the algorithm now deals with the larger MRE with antenna displaced from the measurement center, which can result in longer data acquisition times, especially for high frequency applications and more significant demands in terms of positional accuracy and stability in the measurement system.

A second aspect of the validation is conducted by using time domain (TD) gating. Since a broadband antenna with a short ring-down time is used for this study, TD gating is also possible. At every rotation angle step, the broadband response is inverse Fourier transformed to TD, and a gating function is applied in an attempt to retain the antenna response only without the chamber reflections. The patterns are then reassembled at each frequency and angle using the gated data. In this way, the reference antenna pattern through TD gating can be directly compared to the mode filtered pattern. Lastly, it will be shown that the results from the mode filtering and TD gating processes are indeed comparable. As a result, SVSWR data from the two processes are highly correlatable.

A third aspect of the validation is to compare the results from the proposed method to the traditional CISPR SVSWR results. The CISPR SVSWR results are collected for the requisite positions in the QZ. The mode filtering method shows similar trends, albeit it generally produces more pessimistic results because the CISPR SVSWR is under sampled, and invariably inconsistent.

II. Theoretical Background

In antenna measurement application, the cylindrical mode theory dictates that the step size in radians should not exceed,

$$\Delta\theta = \frac{2\pi}{2[\mathrm{ceil}(k_0\rho_0) + n_1] + 1} \tag{1}$$

where n_1 is an empirical safety factor, e.g., n_1 = 10 [5]; k_0 is the free-space wave number, and ρ_0 is the Maximum Radial Extent (MRE) which is the largest radius to circumscribe the majority of the current sources. Displacing the antenna away from the rotation center has the effect of increasing the electrical size of the antenna, and thus the MRE. The maximum angular step size therefore decreases inversely with frequency. For example, at 18 GHz, for an MRE = 0.5 m, the maximum step size is 0.9°. At 40 GHz, the maximum step size is 0.4°. Similarly, the displacement of the antenna also increases the far-field (FF) distance. The conventional far-field (FF) distance R is given by:

$$R = \frac{2D^2}{\lambda} \approx \frac{8\rho_0^2}{\lambda} \tag{2}$$

where D is the largest dimension of the antenna including the offset, and λ is the wavelength. In the far-field, to translate the antenna to the rotation center, a phase correction is needed:

$$\underline{E}_t(r \to \infty, \theta) = \underline{E}(r \to \infty, \theta) e^{jk_0 \cdot \underline{r}_m} \tag{3}$$

where $\underline{r}_m$ is used to denote the displacement vector between the center of the measurement coordinate system and the center of the current sources (see Fig. 1). In this application, typically, the RSA is 3 m from the QZ edge, and the QZ radius is between 0.5 m and 1 m. Here, the FF condition is clearly not satisfied. A geometric optics (GO) based translation operator was introduced in [1] for the finite range applications such as those encountered in the SVSWR measurements,

$$\underline{E}_t(\theta) = \frac{\underline{E}(\theta)}{R_0} \sqrt{R_0^2 - 2R_0|\underline{r}_m|\cos\theta + |\underline{r}_m|^2}$$
$$e^{jk_0\left(\sqrt{R_0^2 - 2R_0|\underline{r}_m|\cos\theta + |\underline{r}_m|^2} - R_0\right)} \tag{4}$$

Also because of the type of measurement antenna required for the SVSWR measurements (dipole-like and electrically small), this translator proves to be very effective. With the translation applied, the effective MRE is reduced approximately to the radius that encloses the antenna itself as if it is located in the measurement center, rather than on the periphery, offset by $|\underline{r}_m|$. This relaxes the $\Delta\theta$ requirement significantly when recovering the reference antenna pattern CMCs. The chamber multipath effect can still be under sampled, but with a small angular step size such as 1° and collecting samples around the entire QZ perimeter, the under sampling of the chamber environment is not noticeable. This is contrasted to the CISPR measurements, where only 6 samples are collected along a 40 cm line (which is 24λ long at 18 GHz).

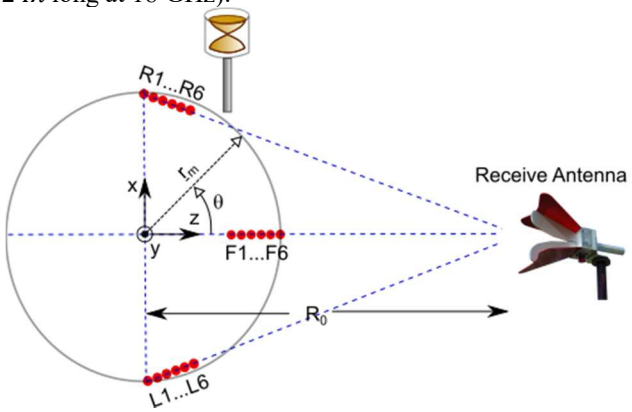

Fig. 1. SVSWR test setup per CISPR 16-1-4.

Fig. 1 shows a plan view of the SVSWR measurement setup. The red dots illustrate the positions needed to measure the CISPR SVSWR. In the mode filtering method, the measurement antenna is positioned at the edge of the turntable, and θ is varied from 0° to 360°. The vector single cut pattern data is then translated to the rotation center based on (4), and the equivalent Cylindrical Mode Coefficients (CMCs) can be obtained using standard cylindrical theory [5],

$$B_n^1 = -\frac{(-j)^{-n}}{4\pi}\int_0^{2\pi} E_\theta(r\to\infty,\theta)e^{-jn\theta}d\theta \tag{5}$$

$$B_n^2 = -\frac{(-j)^{-n}}{4\pi}\int_0^{2\pi} E_\phi(r\to\infty,\theta)e^{-jn\theta}d\theta \tag{6}$$

where $B_n^{1,2}$ are complex CMCs for the TE and TM polarizations; and $E_{\theta,\phi}$ are the electric field components. Notice that the two polarizations are uncoupled, therefore, one set of CMCs can be calculated without the knowledge of the other field component. The calculation also lends itself to the application of the Fast Fourier Transform (FFT) when the angular increment is constant, as is the case here. The CMCs are then filtered to remove the higher order modes to retain only the modes associated with the measurement antenna. Because the modes are generally tightly bounded and separated from contaminants, the results are not particularly sensitive to the selection of the filter function itself. A good candidate is similar to the one used in [7]

$$f = \begin{cases} 0.8^{(|n|-n_{Max})} & \text{when } |n| > n_{Max} \\ 1 & \text{elsewhere} \end{cases} \tag{7}$$

where n is the index of the CMCs, and n_{Max} denotes the highest order modes to encompass the now mathematically centered antenna. The filtered electric field, *i.e.*, the reference pattern, can be calculated through the inverse operation of (5) and (6), typically implemented via an IFFT.

III. Comparison to Quasi-Far-Field Processing

The arrangement depicted in Fig. 1 was used to acquire the experimental data. Fig. 2 shows the actual test setup. The remote source antenna (RSA) used was an ETS-Lindgren Model 3117 double ridged waveguide horn, and the measurement antenna, *i.e.* test antenna, was an ETS-Lindgren Model 3183B omni-directional antenna, both operating from 1-18 GHz. A fresh set of amplitude and phase data was acquired for this paper, as opposed to re-using the data in [1], to ensure the respective algorithms were utilizing the same data acquired using the same test setup.

In the algorithm presented in Section II, a geometrical optics ray-based correction was applied to translate the electrically small antenna to the rotation center. The algorithm was predicated on the assumption that an electrically small antenna is measured at a quasi-far-field distance, and that its propagation behavior can be adequately represented by the far-field representation. In this section, we use an alternative approach where no such assumption is made. It has been shown that a cylindrical wave expansion (CWE) can be used to directly transform the quasi-far-field (QFF) to the true FF from a single-cut pattern [8] providing the antenna is in the far-field in the orthogonal axis. This is applicable to bases-station type antennas [8], or as is the case here, to electrically small antennas that have been offset in a single, azimuthal axis. The QFF condition can be met when only the relatively small antenna dimension itself satisfies the far-field condition. For both TE and TM cases, the mode coefficients C_n can be calculated by [8]:

$$C_n = -\frac{\sqrt{R_0}}{2\pi H_n^{(2)}(k_0R_0)}\int_{-\pi}^{\pi} E_{\theta,\phi}(R_0,\theta)e^{-jn\theta}d\theta \tag{8}$$

where $E_{\theta,\phi}(R_0,\theta)$ is the measured electric field at R_0. During the derivation of (8), the derivative of the Hankel function is approximated by,

$$H_n^{(2)'}(k\rho) \approx -jH_n^{(2)}(k\rho) \tag{9}$$

This is valid for $k\rho \gg (k\cdot \mathrm{MRE} + n_1)$, where n_1 is typically set as 10. The validity of (9) is verified using the experimental data herein. For brevity, the comparison is not shown here. The asymptotic FF pattern can then be calculated from the mode coefficients in the usual way,

$$F_{\theta,\phi}(\theta) = \sum_n C_n j^n e^{jn\theta} \tag{10}$$

The next step is to translate the FF results to the rotation center using (3). Since the result from (10) is for the asymptotic far-field, the application of (3) is exact. The remaining processes including transforming the FF pattern to CMCs, filtering out the higher order modes, and subsequently transforming back to the field remain the same as in Section II.

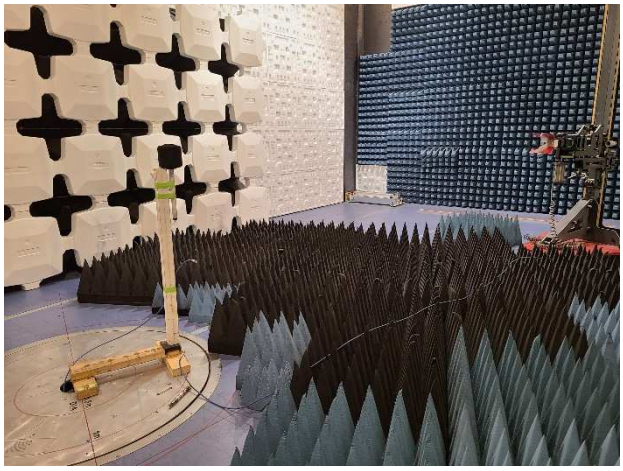

Fig. 2. Test setup used acquire the SVSWR data,

Fig. 3 shows the mode distributions by using the two different algorithms. For the modes close to the antenna, these two methods produce very similar results. For higher order modes, there are some deviations partly because of their different sampling requirements and corresponding band limits. However, as the high order modes differences are filtered out in the processing, they do not affect SVSWR results, which is shown below in Fig. 4. Here it can be seen that the agreement is very favorable at lower frequencies however some differences are evident towards the top of the band, *e.g.* above ~10 GHz. This is likely a consequence of the higher accuracies placed upon the positioning equipment and stability of the

guided-wave path as imposed by the data transformation processing and fine sample spacing that is a direct consequence of the comparatively large MRE.

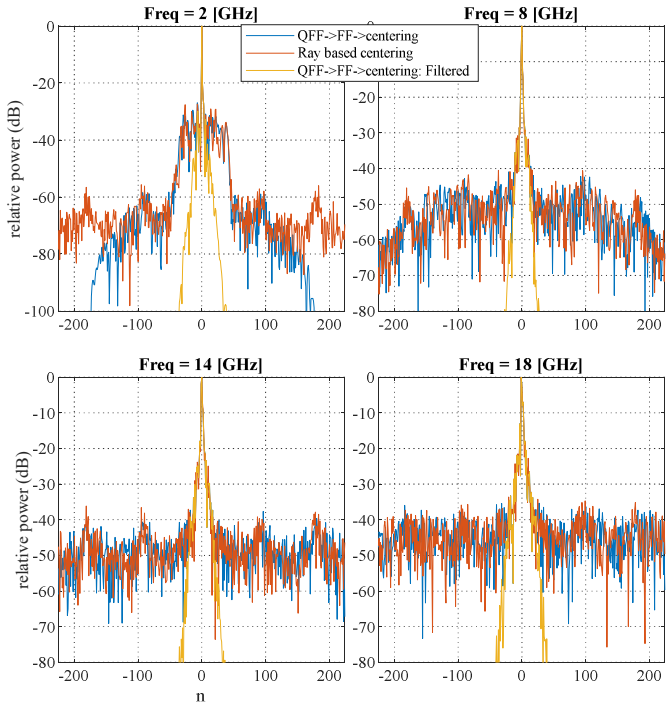

Fig. 3. CMCs using the QFF to FF processing, compared to using the GO based translation at 2, 8, 14 and 18 GHz.

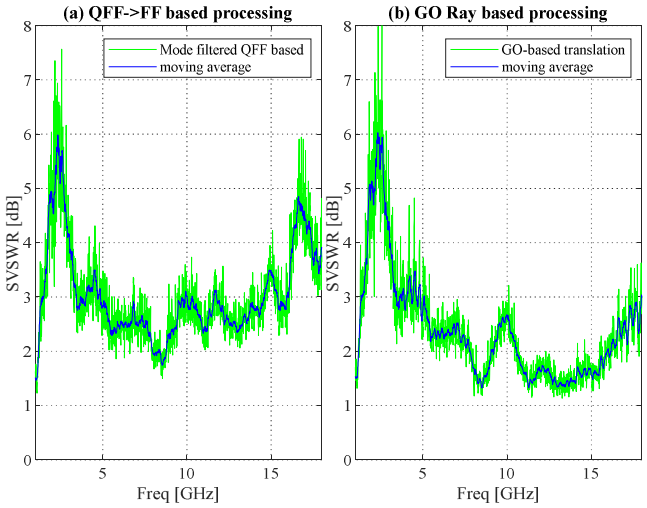

Fig. 4. SVSWR using the QFF to FF processing and using the GO based processing.

IV. Comparison to TD gated results

Both RSA and measurement antennas used for this study were broadband, which makes TD gating also viable. The broadband vector response at each angular step is gated to include only the initial antenna response. TD gated response at each frequency for all the angular steps forms the gated antenna pattern for that particular frequency. The antenna pattern through gating can be compared to the mode filtered pattern as outlined in Section II above (using the GO based processing). As an example, Fig. 5 shows the TD view and the gating of the impulse response for $\theta = 0°$. Here, the same operation was performed at each angular step. Fig. 6 shows the comparison of the resulting reference pattern at frequencies of 2, 8, 14 and 18 GHz. Fig. 7 shows the resulting SVSWR using the gated pattern as the reference. From inspection it can be seen that this compares favorably against Fig. 5(b). The close correlation between both data sets provides additional validation for the mode filtering process.

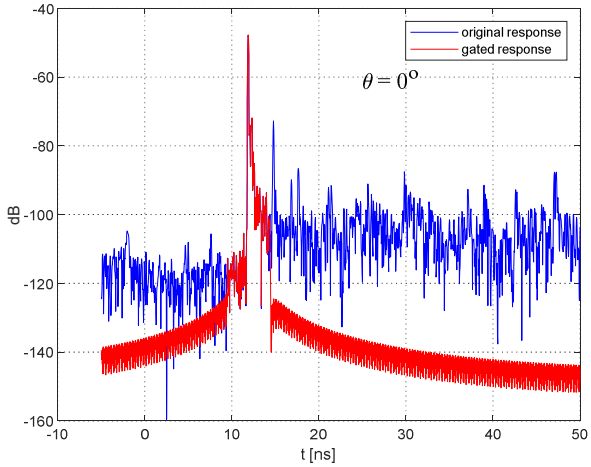

Fig. 5. Time domain view of gating for $\theta = 0°$. Gating is applied for all angular steps. The results are used to form the gated antenna pattern at every frequency.

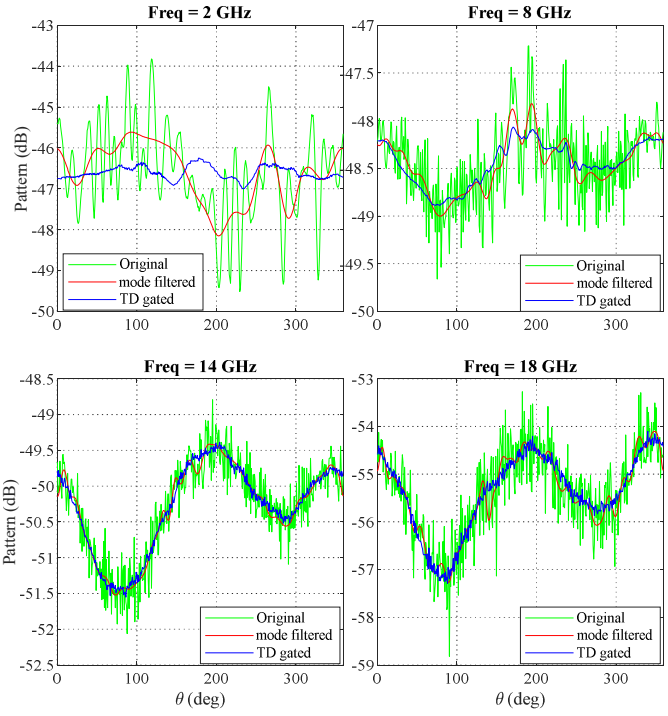

Fig. 6. Reference pattern comparison using mode filtering and TD gating for (a) 2 GHz (b) 8 GHz and (c) 18 GHz

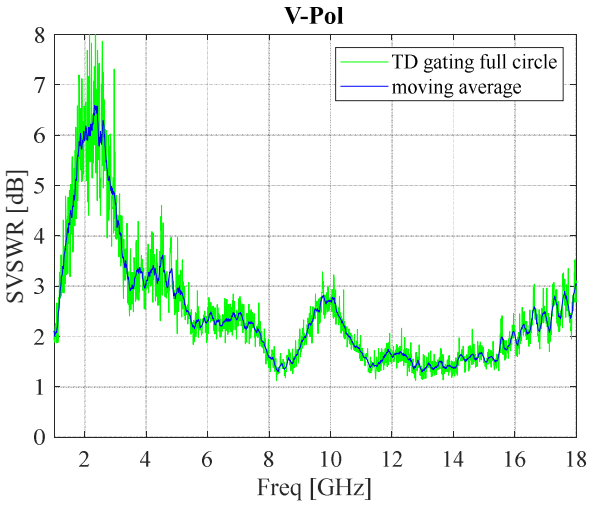

Fig. 7. SVSWR using TD gated antenna pattern as the reference.

Crucially, this is the first time this sort of comparison has been made between time-domain and frequency-domain mode filtering scattering suppression techniques. The agreement between the very different techniques is extremely encouraging as they produce very similar results by utilizing processing in opposite domains, *i.e.* time and frequency.

V. Comparison to Traditional SVSWR

The SVSWR using the traditional CISPR approaches was measured using the same chamber and antenna configuration. Fig. 8 shows the measured SVSWR data using the CISPR method with a frequency interval of 1 MHz (blue curve), and an interval of 50 MHz (which is more commonly used in practice). Fig. 9 shows the measured SVSWR using the TD method specified in ANSI C63.25.1. Here, the C63.25.1 TD SVSWR is calculated from the moving average with an added adjustment, (0.676σ, where σ is the standard deviation within the moving window, as is prescribed by ANSI C63.25.1[3]), which is shown as the blue curves in Fig. 9. The similarity of the trend of these traditional SVSWR results to the mode filtered results, *cf.* Fig. 4(b) is obvious and very encouraging. It is also clear that the mode filtered data are more severe. Both CISPR and TD SVSWR consider only the first half of the QZ by taking measurements for the front, left, and right of the circle, *cf.* Fig 1, whilst Fig. 4(b) considers the entire circle in the calculation. To make the results equivalent, Fig. 10 shows the SVSWR where only the front half of the pattern (-90° to 90° from the boresight) is considered. Here, it is observed that the moving average of the SVSWR using the mode filtering technique aligns with the severity of the current standards remarkably well. For correlation purposes, only the front half of the circle should be used for calculating the SVSWR, although it is debatable whether that constitutes a thorough evaluation of the entire QZ, which is a point that was raised earlier (*cf.* Fig. 10 in [9]).

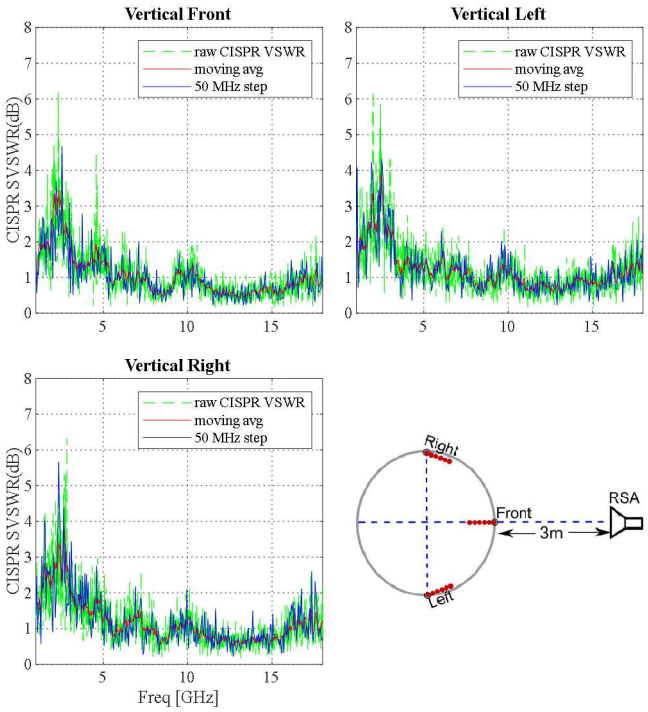

Fig. 8. CISPR SVSWR using the procedure in CISPR 16-1-4.

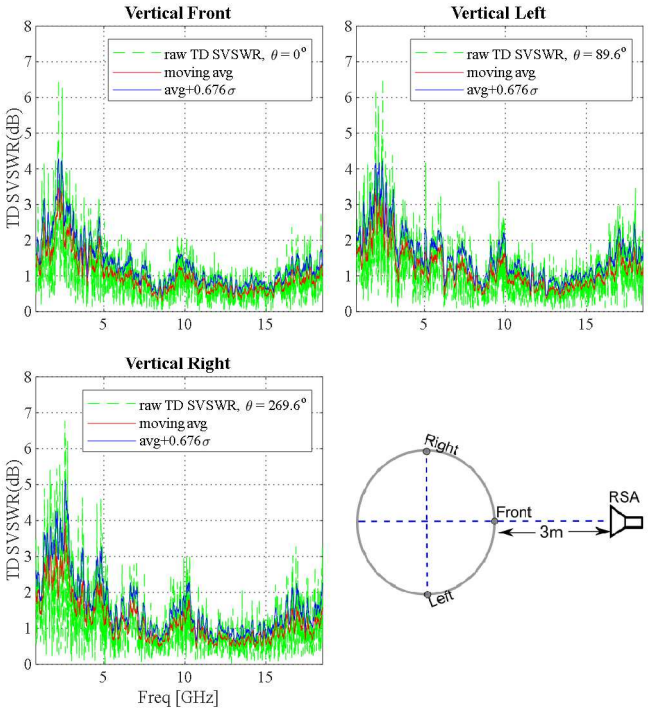

Fig 9. TD SVSWR using the procedure in ANSI C63.25.1.

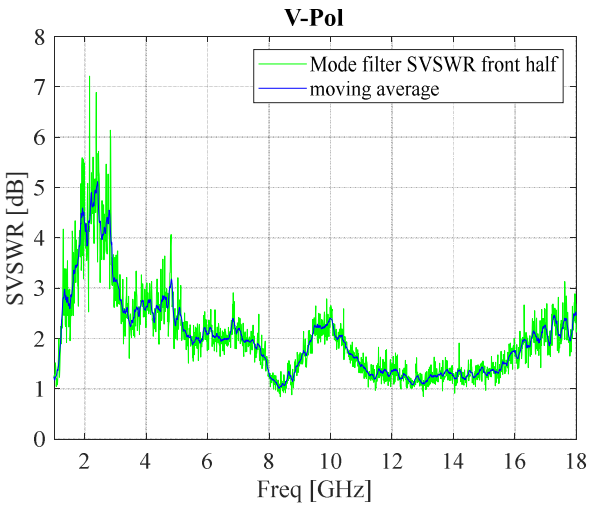

Fig. 10. SVSWR using the mode-filtering method with consideration of the front half of the QZ circle.

VI. Summary and Conclusions

In this paper, a comprehensive study has been conducted to validate the mode filtering technique proposed in [1] for EMC chamber QZ evaluation at above 1 GHz. To validate the ray-based translation of the antenna to its rotation center, a more rigorous algorithm is employed whereby the QFF pattern is first transformed to the FF using SWE before a FF phase adjustment is made to translate antenna to the origin. The close correlation between the two independent methods proves the ray-based approach is accurate for this application with the benefit of reducing sampling requirements and relaxing instrumentation and positioner accuracies. The reference pattern is also obtained through TD gating by taking advantage of the broadband antennas used in this study. The agreement between the time domain processing (gating) and frequency domain processing (mode filtering) further validates the mode filtering technique. Additionally, the SVSWR results from the proposed mode filtering technique is compared to the two traditional SVSWR methods specified in CISPR 16-1-4 and ANSI C63.25.1. It is found that by using the front half of the QZ circle, which matches the traditional SVSWR measurement topography, SVSWR results from the mode filtering method match well with the severity of the current test requirements.

As noted above, this paper recounts the progress of an ongoing study. Consequently, the planned future work is to include examining the impact of parallax error compensation in the ray-based finite range length AUT translation post-processing and the effect of probe compensation on the quasi-far-field to true far-field transform.

Acknowledgment

The authors wish to thank David Macklom at ETS-Lindgren for collecting the measurement data.

References

[1] Z. Chen and S. Gregson, “Examination of EMC Chamber Qualification Methodology for Applications above 1 GHz Using Frequency Domain Mode Filtering”, AMTA 2020.

[2] “Specification for radio disturbance and immunity measuring apparatus and methods - Part 1-4: Radio disturbance and immunity measuring apparatus - Antennas and test sites for radiated disturbance measurements,” CISPR/CIS/A, CISPR 16-1-4:2019, Jan. 2019.

[3] ANSI C63.25.1-2018: American National Standard Validation Methods for Radiated Emission Test Sites, 1 GHz to 18 GHz, 2019.

[4] S. Gregson, et. al., “Application of Mathematical Absorber Reflection Suppression to direct Far-Field antenna range measurements,” in Antenna Measurement Techniques Association Symposium (AMTA), 2011.

[5] C.G. Parini, S.F. Gregson, J. McCormick, D. Janse van Rensburg “Theory and Practice of Modern Antenna Range Measurements”, IET Press, 2014, ISBN 978-1-84919-560-7.

[6] S.F. Gregson, Z. Tian, “Verification of Generalized Far-Field Mode Filtering Based Reflection Suppression Through Computational Electromagnetic Simulation”, IEEE International Symposium on Antennas and Propagation and North American Radio Science Meeting, 5-10 July 2020, Montréal, Québec, Canada.

[7] S. Gregson A.C. Newell, and C.G. Parini, “Verification of Spherical Mathematical Absorber Reflection Suppression in a Combination Spherical Near-Field and Compact Antenna Test Range,” in AMTA symposium 2017.

[8] X. Li, G. Wei, L. Yang, B. Liao, “Fast Determination of Single-Cut Far-Field Patterns of Base Station Antennas at a Quasi-Far-Field Distance”, IEEE Trans. On Antennas and Propagation, Vol. 68, No. 5, May 2020.

[9] Z. Chen and Z. Xiong, "Site contributions for radiated emission measurement uncertainties above 1 GHz," *2017 IEEE International Symposium on Electromagnetic Compatibility & Signal/Power Integrity (EMCSI)*, 2017.